Ionic additive strategy to control nucleation and generate larger single crystals of 3D covalent organic frameworks

Journal:	*ChemComm*
Manuscript ID	CC-COM-04-2021-001857.R1
Article Type:	Communication

SCHOLARONE™
Manuscripts

COMMUNICATION

Ionic additive strategy to control nucleation and generate larger single crystals of 3D covalent organic frameworks

Xiaohan Wang,[a] Riku Enomoto[a] and Yoichi Murakami[a,b]*

To generate large single crystals of 3D covalent organic frameworks, the active use of ionic additives, which can greatly impact crystal size, is proposed. The crystal size ranking was found to be in accordance with the Hofmeister series and Gutmann donor number, providing a useful strategy to enhance crystal size and, consequently, generate COF-300 single crystals of >200 μm in size.

Covalent organic frameworks (COFs) are crystalline porous polymers with 2D or 3D reticulated networks.[1] Since their discovery,[2] the excellent design flexibility of COFs has shown promise in applications including energy storage,[3] catalysis,[4] and drug delivery.[5] Although most efforts in this field have been devoted to 2D-COFs,[1] 3D-COFs are also receiving attention owing to their mechanical flexibility,[6] large internal voids,[7] and topological diversity.[8] Accordingly, significant progress was made in 2018 by Ma et al., who grew 3D imine-bonded single crystalline COFs with sizes of 50–100 μm, readily observable by optical microscope, which were subjected to X-ray structural determination.[6b] This success was made possible by the optimal use of modulators,[9] which were used to implement reversible transimination to correct structural errors.[6b]

The pursuit of further large 3D-COF single crystals is of great interest because it would allow many bulk applications, such as those in which many inorganic crystals are currently used. To realize this, the factors influencing crystal growth need to be elucidated. Although some excellent studies on the nucleation and growth of 2D-COFs have already been reported,[10] such studies on 3D-COFs have yet to be reported. Specifically, a literature search in Web of Science using keywords "covalent organic framework*" and "nucleation*" in the title gave only six results,[§] all of which were related to 2D-COFs.

Identification of the factors influencing crystal growth in other materials is also crucial. Previously, the nucleation and crystal growth of proteins,[11] zeolites,[12] and perovskites[13] were controlled or improved by adding ionic additives, including ionic liquids.[14] However, such an approach has not been applied to the single crystal growth of COFs. Therefore, in this communication, we investigate and report the impact of ionic additives on the crystal growth of a benchmark imine-bonded 3D-COF, COF-300,[15,6b] prepared from terephthaldehyde (BDA, **1**) and tetrakis(4-aminophenyl)methane (TAM, **2**) and using acetic acid as catalyst and aniline (**3**) as modulator (Fig. 1a).

Additives #1−#8 were tested (Fig. 1b), all of which were ionic liquids, except #1. NaCl was not tested owing to very low solubility in the chosen solvent. Notably, some previous reports have used ionic liquids as catalytic solvents for COF growth,[16] but herein they are used as additives (only 2.8 equiv. of **2** and 2.5 mol% of acetic acid; Fig. 1a). Owing to these small amounts, the solubilities of the solutes and yield of COF were only slightly altered, with the ionic liquids mainly serving as nucleation controllers, as discussed later.

All samples were grown in a dark and noiseless Peltier incubator kept at 22±0.5 °C. The sample preparation method was based on that of Ma et al.,[6b] but with some modifications based on our optimizations (see ESI† for experimental details). Solutions were passed through a PTFE membrane filter with 200-nm pores prior to growth. As two standards, #0 and #0' were prepared without additives. The composition of #0 was close to that used by Ma et al.,[6b] but resulted in relatively small sizes with relatively poor reproducibility (approx. 40−60 μm along the c-axis after 7 days). As replacing aqueous acetic acid in #0 with glacial acetic acid in #0' greatly improved both the crystal size and reproductivity, #0' was used as the main reference standard. Therefore, samples #1−#8 were prepared by adding each additive to #0'. Additionally, a control sample (#0'') was prepared, in which decane was used as the additive.
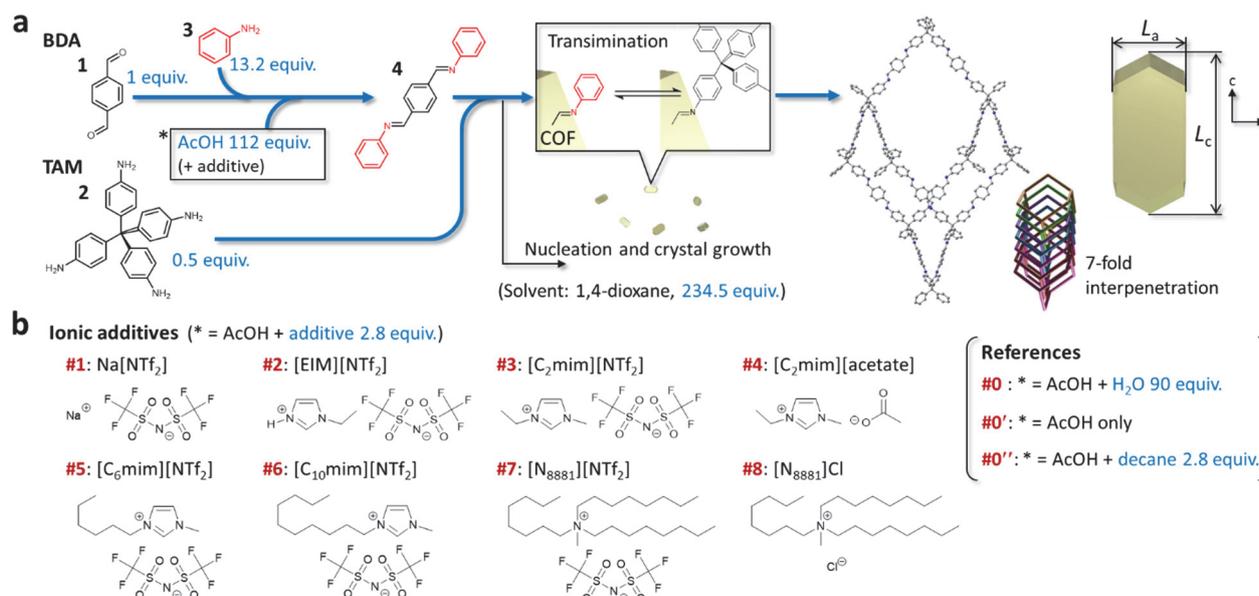
COMMUNICATION

Journal Name

Fig. 1. (a) Scheme of COF-300 synthesis in this study. (b) Molecular structures of additives used in samples #1–#8 and compositions of the three references, #0, #0', and #0'', employed in this study. All molar equivalents written in blue characters are relative to **1**.

Initially, the number of retention days used for growth needed to be selected. The concentration of precursor species **4** (Fig. 1a) in the sample liquid, which emerged after mixing **1** and **3** in dioxane, was conveniently monitored by optical absorption near 350 nm (Fig. 2a). This attribution was confirmed by quantum chemical simulation (Fig. S1a[†]). Two features were noted, as follows. First, before adding **2** (approx. 10 h after mixing **1** and **3**), the absorption measurements showed very similar absorbance for all samples (Fig. S2[†]). This indicated that the formation of **4** was virtually quantitative, probably owing to its exothermic nature.[6b] Second, before and after adding **2** (see Fig. 1a), the sample liquids were transparent without turbidity. Therefore, absorbance evaluations were conducted on solutions, not suspensions. From the temporal curves in Fig. 2b and our observation that retention for 20 days did not greatly enhance sizes (Fig. S3[†]), we determined that 7 days was sufficient. Comparing the absorbance of the liquid at ~350 nm on days 0 and 7, the COF yield on day 7 was estimated, which was similar in all cases (approx. 50±10%, except for #0; Table 1).

On day 7, different additives resulted in different crystal sizes (Fig. 3a). Notably, these results were quantitatively reproducible (see Fig. S4[†] for size distribution histograms of all the experiments conducted three times; see also Fig. 3b). The PXRD patterns of the generated crystals perfectly coincided with that reported for **dia-c7** COF-300 single crystals[6b] (Fig. S5, ESI[†]). The single crystallinity was checked by polarized light microscopy (Fig. S6, ESI[†]). After washing with organic solvents, ionic liquid additives were absent in the pores according to the results of porosity and X-ray fluorescence measurements (Figs. S7 and S8 in ESI[†], respectively).

As these size trends were reproducible, the impact of ionic additives on growth was unequivocal. Furthermore, as the estimated COF yields were similar among all samples, except for #0 (see Table 1), the ionic additives were considered to mainly impact the number of nucleations. Accordingly, Fig. 3a shows

that ionic liquids bearing long alkyl chains, such as [N$_{8881}$][NTf$_2$] and [C$_{10}$mim][NTf$_2$], seemed to suppress nucleation, resulting in larger crystal sizes compared with #0'. In contrast, small ions, such as Na$^+$ and Cl$^-$, seemed to promote nucleation, resulting in smaller crystal sizes compared with #0'. The same tendencies were found also when the original concentrations of **1**, **2**, and aqueous acetic acid in ref. 6b were used, although resulted crystal sizes were much smaller (Fig. S9, ESI[†]). These tendencies implied the existence of some governing rules.

In an attempt to account for these tendencies, a strong correlation between crystal size and the Hofmeister series

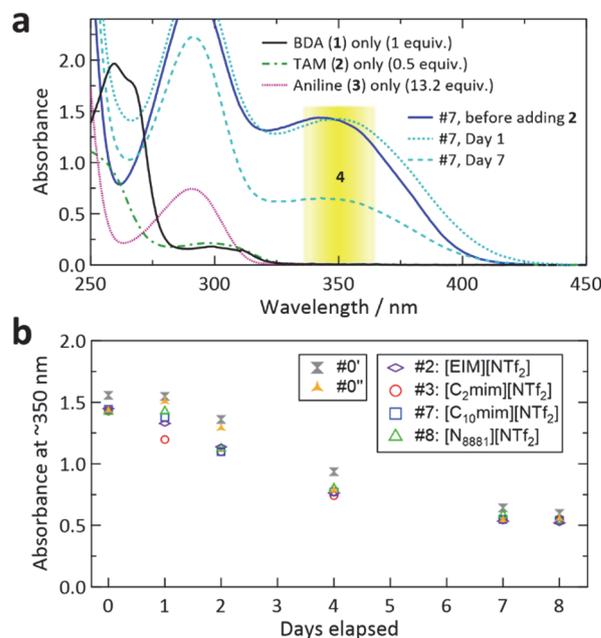**Fig. 2**. (a) Optical absorption spectra (path length, 1 mm) of dioxane solutions of BDA (**1**, 1 equiv.), TAM (**2**, 0.5 equiv.), and aniline (**3**, 13.2 equiv.), all diluted 40-fold with dioxane. (b) Temporal change of peak absorbance at around 350 nm measured for some representative samples in this study. COF yields were estimated using the absorbance on days 0 and 7, as summarized in Table 1, for all samples.

COMMUNICATION

Table 1. Summary of crystal sizes and yields.

	$L_{c,av}{}^a$ (std. dev.) / μm	$L_{a,av}{}^a$ (std. dev.) / μm	Yield^b / %
#0	51.6 (7.9)	28.6 (4.8)	78.6
#0′	96.1 (20.7)	50.5 (12.2)	49.1
#0″	99.2 (19.0)	50.6 (12.2)	57.5
#1	76.8 (13.0)	37.9 (6.8)	39.2
#2	91.9 (15.7)	47.1 (8.9)	58.7
#3	96.2 (17.0)	49.5 (9.5)	57.4
#4	81.2 (13.8)	45.2 (8.2)	60.8
#5	97.8 (18.4)	50.0 (10.8)	59.2
#6	107.2 (16.4)	56.0 (9.5)	60.1
#7	147.6 (23.4)	76.6 (14.8)	56.7
#8	124.9 (17.9)	63.8 (10.0)	53.7

^{a} $L_{c,av}$ and $L_{a,av}$, average crystal dimensions along the c-axis and a-axis, respectively, as determined from 300 crystals in each case after 7 days of growth; see Fig. 3a for photographs and Fig. S4† for size histograms. ^{b} Estimated from absorbance of the solution at around 350 nm after 7 days of growth.

previously reported for ionic liquids,[17] which originally ranked ion-specific effects on protein stability in aqueous environments, was observed. Please note that, herein, EIM$^+$ has been placed between C$_2$mim$^+$ and Na$^+$, in conjunction with the reported Hofmeister order for 1-butylimidazolium$^+$ (BIM$^+$), C$_8$mim$^+$, and C$_2$mim$^+$.[18] Furthermore, N$_{8881}{}^+$ was substituted for N$_{4444}{}^+$ in the original paper,[18] assuming their similarity. This series originated from a report by Hofmeister in 1888, who investigated the relative ability of several inorganic ions to precipitate proteins.[19] Since then, the Hofmeister series has broadly been used to explain, for example, relative effects on the stability and activity of enzymes caused by ionic liquids,[20] and the crystallization of zeolites.[12] Such effects are collectively termed 'Hofmeister effects'[19,21] and are not limited to aqueous media.[22] However, the mechanism of the Hofmeister effect has yet to be elucidated and remains under active investigation.[19,21] Notably, traditional descriptions in terms of the structure of water based on kosmotropic (structure-making) and chaotropic (structure-breaking) concepts[23] have been disproved by experimental and computational evidence of the inability of ions to cause such long-range structure in water.[17,24] Instead,

recent studies have attributed Hofmeister effects to the direct interactions of ions with solute macromolecules and hydration molecules.[17,19,24b]

According to this updated concept of direct ion interactions, which might occur with precursor **4** (see Fig. S1b† for the calculated charge distribution), nascent COF nuclei, and/or solvating molecules around them, our results were evaluated using Gutmann donor and acceptor numbers (DN and AN, respectively),[25] which are a quantitative measure of Lewis basicity and acidity.[26]

A large experimental dataset of DNs with fewer ANs of ionic liquids has been reported by Schmeisser and coworkers.[26] As the DNs of [N$_{8881}$]Cl and [N$_{8881}$][NTf$_2$] have not been reported, they were calculated using a recently reported dataset of their Kamlet–Taft parameters[27] and the conversion relation reported by Marcus.[28] However, no reliable DNs for #1 and #2 were found. As shown in Fig. 3b, a clear correlation was discovered between crystal size and DN for the ionic additives, with three datapoints shown for each condition to represent the extent of reproducibility (see caption for details). Notably, control sample #0″ containing decane exhibited no difference compared with reference #0′, implying that an ionic nature was essential for this phenomenon (considering the DN only to be insufficient). It is known that the DNs of ionic liquids reflect the steric effects of alkyl chains on their cations.[26,27a] No clear correlation with AN was found (Fig. S10†).

The correlation with DN seemed to support the aforementioned hypothesis that the ions provided direct interactions, presumably with precursor **4**, nascent COF nuclei, and/or solvating molecules around them, through some feature related to Lewis basicity. Such interactions were considered to affect nucleation and, therefore, final crystal size, because the estimated COF yields were similar in all cases, except for #0 (Table 1).

Further experimental and theoretical investigation of these mechanisms are beyond the scope of this communication. However, we believe that the above results provide sufficient novel findings, including the discovery that the crystal size
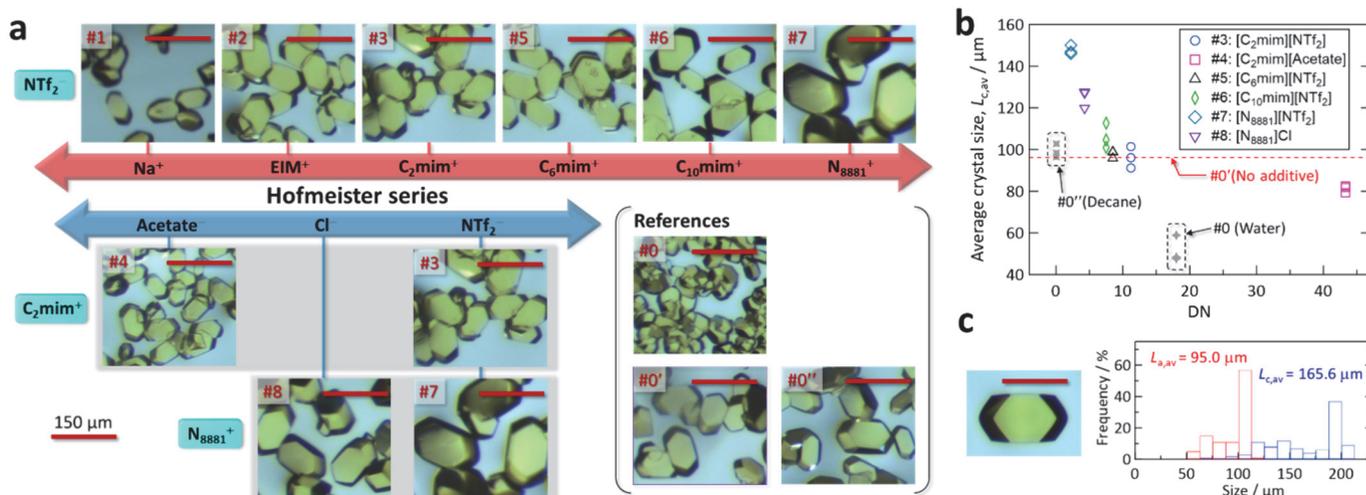

Fig. 3. (a) Optical micrographs (bar, 150 μm) after 7 days of crystal growth in solution, displayed in order of the Hofmeister series of cations and anions. (b) Plot of average sizes along the c-axis against DNs of additives. DNs of water and decane are from ref. 28. Three datapoints are shown for each condition to obtain reproducibility, with each datapoint as an average of 100 crystals; see Fig. S4† for all size histograms from which these datapoints were generated. (c) Optical micrograph (bar, 150 μm) of a crystal >200 μm in size along the c-axis grown for 7 days with #7 (1.9 equiv., see Fig. S11†) and the size histogram of this sample.

tendency is in agreement with the Hofmeister series and correlates with Guttman DNs. Finally, the dependence of crystal size on the amount of our best additive, $[N_{8881}][NTf_2]$, was found to be weak (Fig. S11[†]). However, thanks to this slight optimization, crystals with sizes >200 μm were obtained (Fig. 3c), which is the largest single crystal reported for imine-based 3D-COFs to date. Overall, the results and mechanistic findings presented in this study provide important clues for enhancing single crystal sizes, which will aid the exploration of applications where using COFs as macroscale crystalline materials.

Notes and references

§ https://apps.webofknowledge.com/, as of April 2021.

1   (*a*) C. S. Diercks and O. M. Yaghi, *Science*, 2017, **355**, eaal1585; (*b*) R. P. Bisbey and W. R. Dichtel, *ACS Cent. Sci.*, 2017, **3**, 533–543.

2   (*a*) A. P. Côté, A. I. Benin, N. W. Ockwig, M. O'Keeffe, A. J. Matzger and O. M. Yaghi, *Science*, 2005, **310**, 1166–1170; (*b*) H. M. El-Kaderi, J. R. Hunt, J. L. Mendoza-Cortés, A. P. Côté, R. E. Taylor, M. O'Keeffe and O. M. Yaghi, *Science*, 2007, **316**, 268–272.

3   (*a*) R. DeBlase, K. E. Silberstein, T. T. Truong, Héctor H. D. Abruña and W. R. Dichtel, *J. Am. Chem. Soc.*, 2013, **135**, 16821–16824; (*b*) H. Liao, H. Ding, B. Li, X. Ai and C. Wang, *J. Mater. Chem. A*, 2014, **2**, 8854–8858; (*c*) C. R. Mulzer, L. Shen, R. P. Bisbey, J. R. McKone, N. Zhang, H. D. Abruña and W. R. Dichtel, *ACS Cent. Sci.*, 2016, **2**, 667–673; (*d*) Y. Meng, G. Lin, H. Ding, H. Liao and C. Wang, *J. Mater. Chem. A*, 2018, **6**, 17186–17191; (*e*) A. F. M. EL-Mahdy, M. G. Mohamed, T. H. Mansoure, H. H. Yu, T. Chen and S. W. Kuo, *Chem. Commun.*, 2019, **55**, 14890–14893.

4   (*a*) Q. Fang, S. Gu, J. Zheng, Z. Zhuang, S. Qiu and Y. Yan, *Angew. Chem. Int. Ed.*, 2014, **53**, 2878 –2882; (*b*) X. Wang, X. Han, J. Zhang, X. Wu, Y. Liu and Y. Cui, *J. Am. Chem. Soc.*, 2016, **138**, 12332–12335; (*c*) Y. Li, W. Chen, R. Gao, Z. Zhao, T. Zhang, G. Xing and L. Chen, *Chem. Commun.*, 2019, **55**, 14538–14541; (d) J. C. Shen, W. L. Jiang, W. D. Guo, Q. Y. Qi, D. L. Ma, X. Lou, M. Shen, B. Hu, H. B. Yang and X. Zhao, *Chem. Commun*., 2020, **56**, 595–598.

5   (*a*) Q. Fang, J. Wang, S. Gu, R. B. Kaspar, Z. Zhuang, J. Zheng, H. Guo, S. Qiu and Y. Yan, *J. Am. Chem. Soc.*, 2015, 137, 8352–8355; (*b*) L. Bai, S. Z. F. Phua, W. Q. Lim, A. Jana, Z. Luo, H. P. Tham, L. Zhao, Q. Gao and Y. Zhao, *Chem. Commun.*, 2016, **52**, 4128–4131; (*c*) Q. Guan, L. L. Zhou, W. Y. Li, Y. A. Li and Y. B. Dong, *Chem. Eur. J.*, 2020, **26**, 5583–5591.

6   (*a*) Y. X. Ma, Z. J. Li, L. Wei, S. Y. Ding, Y. B. Zhang and W. Wang, *J. Am. Chem. Soc.*, 2017, **139**, 4995–4998; (*b*) T. Ma, E. A. Kapustin, S. X. Yin, L. Liang, Z. Zhou, J. Niu, L. H. Li, Y. Wang, J. Su, J. Li, X. Wang, W. D. Wang, W. Wang, J. Sun and O. M. Yaghi, *Science*, 2018, **361**, 48–52; (*c*) Y. Chen, Z. L. Shi, L. Wei, B. Zhou, J. Tan, H. L. Zhou and Y. B. Zhang, *J. Am. Chem. Soc.*, 2019, **141**, 3298–3303.

7   (*a*) B. Gui, G. Lin, H. Ding, C. Gao, A. Mal and C. Wang, *Acc. Chem. Res.*, 2020, **53**, 2225–2234; (*b*) Y. Wang, Y. Liu, H. Li, X. Guan, M. Xue, Y. Yan, V. Valtchev, S. Qiu and Q. Fang, *J. Am. Chem. Soc.*, 2020, **142**, 3736–3741; (*c*) L. Liang, Y. Qiu, W. D. Wang, J. Han, Y. Luo, W. Yu, G. L. Yin, Z. P. Wang, L. Zhang, J. Ni, J. Niu, J. Sun, T. Ma and W. Wang, *Angew. Chem. Int. Ed.*, 2020, **59**, 17991–17995.

8   (*a*) X. Kang, X. Han, C. Yuan, C. Cheng, Y. Liu and Y. Cui, *J. Am. Chem. Soc.*, 2020, **142**, 16346–16356. (*b*) C. Gropp, T. Ma, N. Hanikel and O. M. Yaghi, *Science*, 2020, **370**, eabd6406; (*c*) H. L. Nguyen, C. Gropp, Y. Ma, C. Zhu and O. M. Yaghi, *J. Am. Chem. Soc.*, 2020, **142**, 20335–20339.

9   M. Calik, T. Sick, M. Dogru, M. Döblinger, S. Datz, H. Budde, A. Hartschuh, F. Auras and T. Bein, *J. Am. Chem. Soc.*, 2016, **138**, 1234–1239.

10 (*a*) B. J. Smith, A. C. Overholts, N. Hwang and W. R. Dichtel, *Chem. Commun.*, 2016, **52**, 3690–3693; (*b*) H. Li, A. D. Chavez, H. Li, H. Li, W. R. Dichtel and J. L. Brédas, *J. Am. Chem. Soc.*, 2017, **139**, 16310–16318; (*c*) I. Castano, A. M. Evans, H. Li, E. Vitaku, M. J. Strauss, J. L. Brédas, N. C. Gianneschi and W. R. Dichtel, *ACS Cent. Sci.*, 2019, **5**, 1892–1899; (*d*) H. Li, A. M. Evans, I. Castano, M. J. Strauss, W. R. Dichtel and J. L. Bredas, *J. Am. Chem. Soc.*, 2020, **142**, 1367–1374.

11 R. A. Judge, S. Takahashi, K. L. Longenecker, E. H. Fry, C. Abad-Zapatero and M. L. Chiu, *Cryst. Growth Des.*, 2009, **9**, 3463–3469.

12 (*a*) A. Toktarev and G. V. Echevaskii, *Stud. Surf. Sci. Catal. A*, 2008, **174**, 167–172; (*b*) C. Sun, Z. Liu, S. Wang, H. Pang, R. Bai, Q. Wang, W. Chen, A. Zheng, W. Yan and J. Yu, *CCS Chem.*, 2021, **3**, 189–198.

13 J. Y. Seo, T. Matsui, J. Luo, J. Pp Correa-Baena, F. Giordano, M. Saliba, K. Schenk, A. Ummadisingu, K. Domanski, M. Hadadian, A. Hagfeldt, S. M. Zakeeruddin, U. Steiner, M. Grätzel and A. Abate, *Adv. Energy Mater.*, 2016, **6**, 1600767-1–1600767-6.

14 N. V. Plechkova and K. R. Seddon, *Chem. Soc. Rev.*, 2008, **37**, 123–150.

15 F. J. Uribe-Romo, J. R. Hunt, H. Furukawa, C. Klöck, M. O'Keeffe and O. M. Yaghi, *J. Am. Chem. Soc.*, 2009, **131**, 4570–4571.

16 (*a*) X. Guan, Y. Ma, H. Li, Y. Yusran, M. Xue, Q. Fang, Y. Yan, V. Valtchev and S. Qiu, *J. Am. Chem. Soc.*, 2018, **140**, 4494–4498; (*b*) L. Zhao, H. Liu, Y. Du, X. Liang, W. Wang, H. Zhao and W. Li, *New J. Chem.*, 2020, **44**, 15410–15414.

17 H. Weingärtner, C. Cabrele and C. Herrmann, *Phys. Chem. Chem. Phys.*, 2012, **14**, 415–426.

18 H. Vila-Real, A. J. Alfaia, J. N. Rosa, P. M. P. Goisa, M. E. Rosa, A. R. T. Caladoa and M. H. Ribeiro, *J. Biotech.*, 2011, **152**, 147–158.

19 A. Salis and B. W. Ninham, *Chem. Soc. Rev.*, 2014, **43**, 7358–7377.

20 (*a*) H. Zhao, O. Olubajo, Z. Song, A. L. Sims, T. E. Person, R. A. Lawal and L. A. Holley, *Bioorg Chem.*, 2006, **34**, 15–25; (*b*) H. Zhao, *J. Chem. Technol. Biotechnol.*, 2016, **91**, 25–50.

21 (*a*) W. Kunz, P. L. Nostro, B. W. Ninham, *Curr. Opin. Colloid Interf. Sci.*, 2004, **9**, 1–18; (*b*) Z. Yang, *J. Biotech.*, 2009, **144**, 12–22.

22 N. Peruzzi, B. W. Ninham, P. L. Nostro and P. Baglioni, *J. Phys. Chem. B*, 2012, **116**, 14398–14405.

23 H. Zhao, *J. Chem. Tech. Biotech.*, 2006, **81**, 877–891.

24 (*a*) A. W. Omta, M. F. Kropman, S. Woutersen and H. J. Bakker, *Science*, 2003, **301**, 347–349; (*b*) D. J. Tobias and J. C. Hemminger, *Science*, 2008, **319**, 1197–1198.

25 V. Gutmann, *Electrochim. Acta*, 1976, **21**, 661–670.

26 M. Schmeisser, P. Illner, R. Puchta, A. Zahl and R. van Eldik, *Chem. Eur. J.*, 2012, **18**, 10969–10982.

27 (*a*) G. Thielemann and S. Spange, *New J. Chem.*, 2017, **41**, 8561–8567; (*b*) S. Spange, C. Lienert, N. Friebe and K. Schreiter, *Phys. Chem. Chem. Phys.*, 2020, **22**, 9954–9966.

28 Y. Marcus, *Chem. Soc. Rev.*, 1993, **22**, 409–416.